Electronic relaxation of deep bulk trap and interface state in ZnO ceramics*

Yang Yan(杨 雁)[a], Li Sheng-Tao(李盛涛)[a]†,
Ding Can(丁 璨)[a], and Cheng Peng-Fei(成鹏飞)[b]

[a] *State Key Laboratory of Electrical Insulation and Power Equipment, Xi'an Jiaotong University, Xi'an* 710049, *China*
[b] *School of Science, Xi'an Polytechnic University, Xi'an* 710048, *China*

(Received 25 May 2010; revised manuscript received 3 August 2010)

This paper investigates the electronic relaxation of deep bulk trap and interface state in ZnO ceramics based on dielectric spectra measured in a wide range of temperature, frequency and bias, in addition to the steady state response. It discusses the nature of net current flowing over the barrier affected by interface state, and then obtains temperature-dependent barrier height by approximate calculation from steady I–V (current–voltage) characteristics. Additional conductance and capacitance arising from deep bulk trap relaxation are calculated based on the displacement of the cross point between deep bulk trap and Fermi level under small AC signal. From the resonances due to deep bulk trap relaxation on dielectric spectra, the activation energies are obtained as 0.22 eV and 0.35 eV, which are consistent with the electronic levels of the main defect interstitial Zn and vacancy oxygen in the depletion layer. Under moderate bias, another resonance due to interface relaxation is shown on the dielectric spectra. The DC-like conductance is also observed in high temperature region on dielectric spectra, and the activation energy is much smaller than the barrier height in steady state condition, which is attributed to the displacement current coming from the shallow bulk trap relaxation or other factors.

Keywords: ZnO, deep bulk trap, interface state, relaxation

PACS: 52.25.Mq, 71.15.–m, 77.22.Gm **DOI:** 10.1088/1674-1056/20/2/025201

1. Introduction

ZnO ceramics have been widely used for over voltage protection and surge absorption in power systems, because of the excellent non-linear I–V (current–voltage) characteristics, which were arising from back to back Schottky barrier at grain boundary.[1−3] At grain boundary interface, large amounts of negative charges are trapped by interface states, which are originated from impurities segregation, dislocations and dangling bonds. For electric neutrality, positively charged depletion layers appear on both sides of grain boundary interface, forming the back to back Schottky barrier.[1] As varieties of defects[4,5] existed in ZnO ceramics are due to the inherent non-stoichiometry, the distribution of both positively and negatively charged defects in grain boundary region is rather complicated. Complex electronic structure and defects distribution have a great effect on the electronic behaviour in grain boundary region, but it is difficult to detect and represent.

From the current flowing over the Schottky barrier measured by small current ($j < 10^{-4}$ A/cm^2) DC characteristics of ZnO ceramics, we can obtain steady-state parameters such as the grain boundary barrier height and interface state density.[6] But the effect of the electron trapping and emitting by interface states cannot be obtained, even a two-step electron transportation model is considered.[7−10] While from the dynamic response, more parameters about charged carriers, such as their density, energy level and capture cross section can be obtained.[11,12]

Different from the deep level transient spectroscopy and thermally stimulated current measurements, the broadband dielectric spectroscopy has advantages of wide measuring temperature and frequency range, simplicity and nondestructive nature. Moreover, information about deep bulk trap and interface state, such as trap density, capture cross section, activation energy and relaxation time can all be calculated from the dielectric spectra.[13−15] So broadband dielectric spectroscopy becomes an important means of investigating electronic behaviour of grain boundary.[16]

It was found that a significant loss peak near the frequency of 10^5 Hz appeared on the dielectric spectra

*Project supported by the National Outstanding Young Investigator Grant of China (Grant No. 50625721) and the National Natural Science Foundation of China (Grant No. 50972118).

†Corresponding author. E-mail: sli@mail.xjtu.edu.cn

© 2011 Chinese Physical Society and IOP Publishing Ltd

of ZnO ceramics.[17−19] This loss peak does not depend on specific formula and process of the ceramics, but depends on the composition and defect structure of grain boundaries.[15] In this paper, the additional currents rising from relaxation of deep bulk trap at depletion layer edge were analysed, which is responsible for the loss peak. Then the main defect in the depletion layer was regarded as native defect interstitial Zn and vacancy oxygen based on the activation energies obtained from the resonance on dielectric spectra. Furthermore, interface state relaxation and DC like conductance were also detected from dielectric spectra.

This paper provided a convenience way to represent deep bulk trap, and to reveal the effects of deep bulk trap and interface state on the dielectric properties of ZnO ceramics. After these effects are controlled properly, lots of problems in engineering application can be solved, including reduction residual voltage and improvement of degradation properties.

2. Experiment

In this paper, the sample is commercial ZnO ceramics consisting of ZnO (97 mol%), Bi_2O_3 (0.5 mol%), MnO (0.5 mol%), CoO (1 mol%) and Sb_2O_3 (1 mol%). The specimens were 10 mm in diameter by approximately 1-mm thick. The surfaces were cleaned by using an ultrasonic cleaner before gold electrodes were sputtered on each side of the specimens by vacuum evapouration.

The current–voltage characteristics were measured at various temperatures in an Environmental Test Chamber (DELTA 9023), and an HP 34001A digital multimeter was used to read the current. The dielectric spectra of the sample were measured from 0.1 Hz to 10^7 Hz, –160 °C to 200 °C, and bias from 0 V to 40 V by Broadband Dielectric and Impedance Spectroscopy (Novocontrol).

3. Results and discussion

3.1. Steady-state properties

Figure 1 shows the current–voltage curves of ZnO ceramics from 90 °C to 200 °C. The curves are nonlinear, and the nonlinear coefficient $a = 1/\log(U_{1\ \mathrm{mA}}/U_{0.1\ \mathrm{mA}})$ decreases from 5.61 (90 °C) to 2.77 (200 °C), which is not high enough to consider the tunneling effect[20,21] in the measuring current and temperature region, but comes from the thermionic emission current cross the Schottky barrier in the grain boundary region.

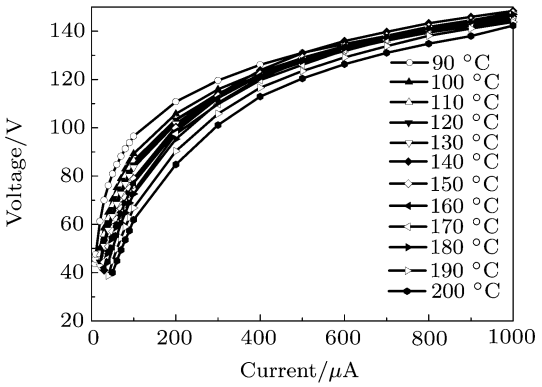


Fig. 1. Current–voltage curves of ZnO ceramics from 90 °C to 200 °C

3.2. Nature of steady-state current in ZnO ceramics

Negative charges are trapped at grain boundary interface, where the energy band bending occurs, forming back to back Schottky barrier. Figure 2 shows the schematic energy band diagram of Schottky barrier when the applied voltage is zero, where E_c, E_0, E_d, E_F and E_v are the bottom of conduction band, shallow donor level, deep donor level, Fermi level and the top of valence band, respectively.

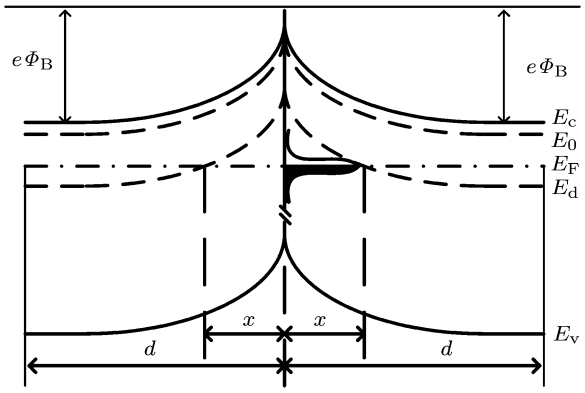


Fig. 2. Schematic energy band diagram of symmetric Schottky barrier.

The barrier is symmetric, and the quasi-Fermi level of interface is the same as the bulk Fermi level. The barrier height Φ_B and width of depletion layer x_0 can be obtained by solving the Poisson's equation including interface charge[1]

$$\Phi_B(V=0) = \frac{Q_i^2}{8e\varepsilon\varepsilon_0 n_0}, \tag{1}$$

$$x_0 = \frac{Q_i}{2n_0} = \left(\frac{2e\varepsilon\varepsilon_0\Phi_B}{n_0}\right)^{1/2}, \tag{2}$$

where Q_i is interface charge, n_0 is density of shallow donor, e is electron charge, ε_0 is permittivity of vac-

uum and ε is the relative permittivity of the dielectric.

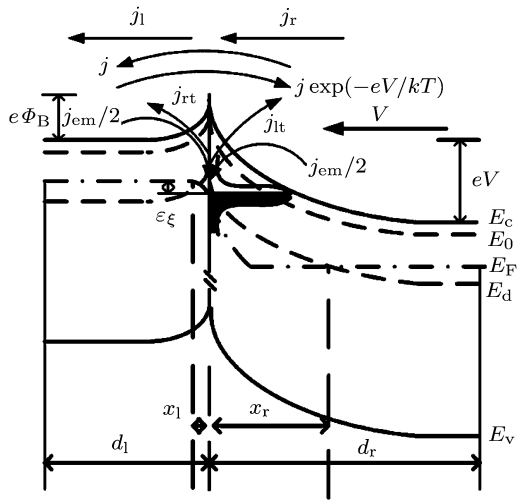


Fig. 3. Schematic energy band diagram of Schottky barrier. It shows the forward thermionic emission current j, reverse current $j\exp(-eV/kT)$, trapped current from the right side $j_{\rm rt}$ and the left side $j_{\rm lt}$ by interface states, and re-emitted current to both sides by interface states $j_{\rm em}/2$ when voltage V is applied across the barrier.

When the applied voltage is not zero, the barrier is no longer symmetric, as shown in Fig. 3. The interface states are in quasi-equilibrium state, and the capture probability can still be expressed by the Fermi distribution function, but a difference appears between the quasi-Fermi level of the interface and the bulk Fermi level, which is determined by balance condition: the number of electrons trapped and the electrons emitted from the interface should be the same.[16] Considering this difference, the relationship between the thermionic emission current density flowing over the barrier and the applied voltage can be written as

$$j = A^* T^2 \exp[-(e\Phi_{\rm B}(V) + \varepsilon_\xi)/kT], \tag{3}$$

where A^* is Richardson's constant, ε_ξ is the difference between the quasi-Fermi level of the interface and the bulk Fermi level, T is absolute temperature.

As electrons transport from one grain into another in a two-step way, interface trapping and emitting should be involved during the electronic transportation process. Now we discuss the details about the net current flowing over the barrier affected by interface state in steady state condition.

As shown in Fig. 3, the current on the left side of the barrier $j_{\rm lb}$ consists of four components: thermionic emission current from left to right j, from right to left $j\exp(-eV/kT)$, the small currents of electrons being trapped from the right-side $j_{\rm rt}$ and re-emitted to the left side from the interface states $j_{\rm em}/2$, assuming that emission from interface states is isotropic, thus we can write the left side current as

$$j_{\rm lb} = j(1 - \exp(-eV/kT)) - j_{\rm em}/2 + j_{\rm rt}. \tag{4}$$

In the same way, the right-side current can be written as

$$j_{\rm rb} = j(1 - \exp(-eV/kT)) + j_{\rm em}/2 - j_{\rm lt}. \tag{5}$$

The trapped current $j_{\rm t} = j_{\rm lt} + j_{\rm rt}$ depends on the electron capture cross section of interface $c(E)$,

$$j_{\rm t} = j(1 + \exp(-eV/kT)) \times \int {\rm d}E c(E) N_{\rm i}(E)(1 - f_{\rm i}(E)). \tag{6}$$

The emission current out of interface state is determined by charge emission rate $b(E)$

$$j_{\rm em} = \int {\rm d}E b(E) \exp(-(E_{\rm b} - E)/kT) N_{\rm i}(E) f_{\rm i}(E), \tag{7}$$

where $E_{\rm b} - E$ is the activation energy for thermionic emission out of the interface.

However, the interface state capture cross section is very small ($\sim 10^{-16}$ cm^2) in ZnO ceramics, thus the effect of interface capture can be ignored in steady state condition.[12] Note that $j_{\rm lb} - j_{\rm rb} = j_{\rm t} - j_{\rm em} = j_{\rm i}$, thus in steady state, the interface current is zero. When $eV \gg kT$, the reverse current can also be ignored. The net current through the barrier can be approximated as j in Eq. (3). In addition, the difference ε_ξ is comparable to kT, and therefore can be ignored in approximate calculation,[6] so the net current flowing over the barrier in steady-state condition can be approximately written as

$$j_{\rm dc} \approx j = AT^2 \exp[-e\Phi_{\rm B}(V)/kT]. \tag{8}$$

According to the Schottky thermionic emission theory, the relationship between effective barrier height and applied electric field can be expressed as $\Phi_{\rm B}(E) = \Phi_0 - \beta\sqrt{E}$, then the static current is[22]

$$j \approx AT^2 \exp\left(-\frac{\Phi_0 - \beta\sqrt{E}}{kT}\right), \tag{9}$$

where A is Richardson constant, T is absolute temperature, k is Boltzmann's constant, Φ_0 is the barrier height when the applied voltage is zero, β is a constant dependent on the material itself. At a fixed temperature, the $\ln j \sim \sqrt{E}$ curve should be linear, and the value of $\ln j_0$ can be obtained from the intercept. After values of $\ln j_0$ at all temperatures are obtained, Φ_0 can be obtained from the slope of $\ln j_0 \sim 1/T$, according to Eq. (9), and ignoring the change of Φ_0 with temperature.

The experimental $\ln j_0 \sim 1/T$ curve is shown in Fig. 4, where the dashed line is the experimental result and the solid lines are linear fitting in two temperature regions.

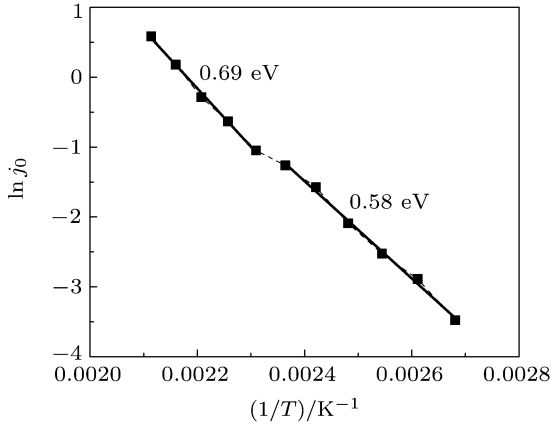


Fig. 4. The $\ln j_0 \sim 1/T$ curve (dashed line) of ZnO ceramics. Where j_0 are obtained from the intercept of the linear fitting line of $\ln j \sim \sqrt{E}$ curve at temperature from 90 °C to 20 °C. From the slope of linear fitting line of $\ln j_0 \sim 1/T$ curve (solid line), the temperature-dependent barrier height can be obtained.

The value of Φ_0 is 0.69 eV in the temperature range of 160 °C∼200 °C, and is 0.58 eV in the temperature range of 100 °C∼150 °C. The $\ln j_0 \sim 1/T$ curve is split into two straight lines, because the assumption that Φ_0 will not change with temperature is no longer satisfied in the whole temperature range. The change of Φ_0 with temperature is rather complicated, since it depends on various parameters such as dielectric constant, the density of interface state and the temperature-dependent interface quasi-Fermi level.[10]

In summary, from the steady state characteristics of ZnO ceramics, we can obtain that Φ_0 decreases with decreasing temperature, the interface current is zero, and the interface capture current is too small to be detected.

The current in breakdown region is quite different from the condition in pre-breakdown region, and we will not discuss it in this paper.

3.3. Dynamic response dielectric spectra

As a small AC signal $V(t) = V_0 + V\mathrm{e}^{\mathrm{i}\,\omega t}$, $eV \ll kT$ is applied across the grain boundary, the interface charge and depletion layer charge become time-dependent. The complex admittance $Y = G + \mathrm{i}\,\omega C$ depends on frequency, temperature and bias, and is affected by deep bulk trap and interface states.

As $\sigma_{\mathrm{DC}} \propto \exp(-E_{\mathrm{a}}/kT)$, from the relationship between conductance G and temperature T, we can easily obtain the information about DC-like conductance. In addition, the information about relaxation can also be obtained from the relationship between conductance and temperature at different frequencies and biases as shown in Fig. 5. So in this paper, the dielectric spectra are figured in the form of the relationship between conductivity and temperature.

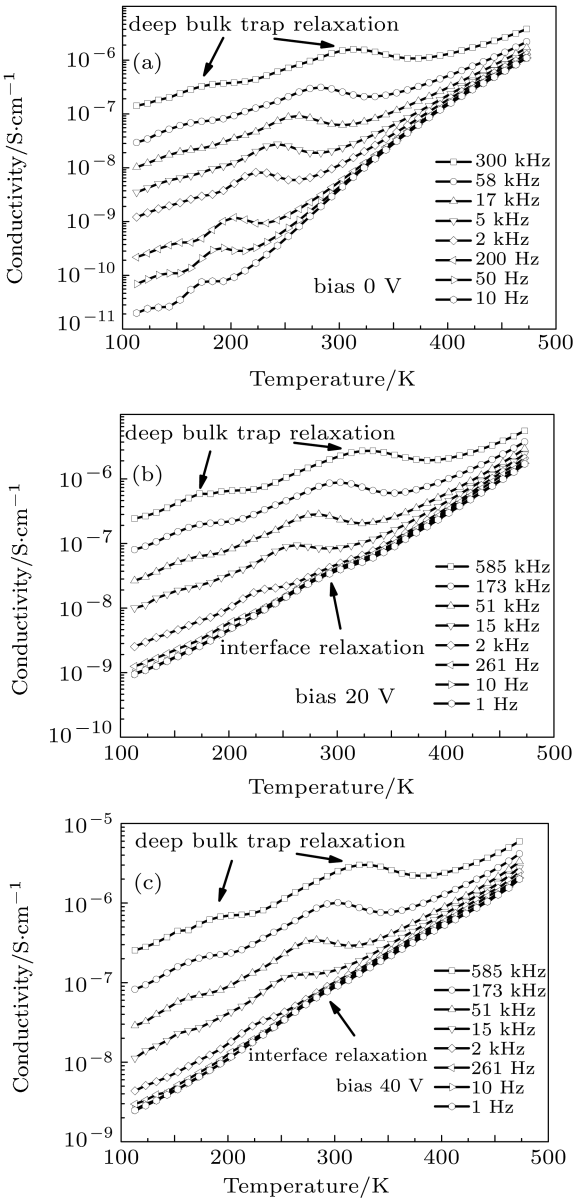


Fig. 5. Relationship between conductivity and temperature at different frequencies when the bias is (a) 0 V, (b) 20 V, and (c) 40 V. Deep bulk trap and interface relaxation are indicated.

3.4. Relaxation of deep bulk trap

When the bias V_0=0, the shape of the barrier is still symmetric, but the cross point position x of the deep bulk trap and Fermi level appear to have a small displacement under AC signal, leading an additional current j_{d} as shown in Fig. 6.[23]

When the voltage increases from V to $V' = V + \mathrm{d}V$, the cross point on the left side of the barrier moves away from the interface, from x to $x' = x + \mathrm{d}x$, part of the traps thereby shifts above the Fermi level, emits electrons. While the voltage decreases again, the

opposite occurs. The situation is the opposite on the right side. Under AC signal, electrons emitting and trapping by deep bulk trap lead an additional current $j_{\rm d}$.

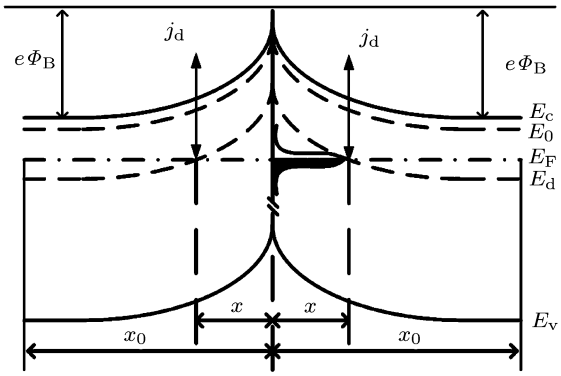


Fig. 6. Schematic diagram of deep bulk trap relaxation under zero bias small AC signal. Additional current rising from deep bulk trap relaxation $j_{\rm d}$ is indicated.

The charge emitted due to the displacement from x to $x' = x + {\rm d}x$ can be written as

$$ {\rm d}Q = eN_{\rm d}A{\rm d}x, \tag{10}$$

where e is electron charge, $N_{\rm d}$ is deep bulk trap density and A is the barrier area.

As the emitting and trapping electrons always occur at the edge of the depletion layer, ${\rm d}x$ can be approximated to ${\rm d}x_0$, namely the change of the width of depletion layer. Considering the effect of the deep bulk trap on carrier density, ${\rm d}x_0$ can be written as

$$ x_0 = \left(\frac{2\varepsilon\varepsilon_0 \Phi_{\rm B}}{eN_+}\right)^{1/2}. \tag{11}$$

By deriving the integrated Poisson equation, we can obtain[23]

$$ {\rm d}x_0 = \frac{{\rm d}V}{x_0}\frac{\varepsilon\varepsilon_0}{en_0}. \tag{12}$$

Thus

$$ {\rm d}Q = \frac{eN_{\rm d}A}{n_0}\left(\frac{\varepsilon\varepsilon_0 N_+}{2e\Phi_{\rm B}}\right)^{1/2}{\rm d}V, \tag{13}$$

where, n_0 is the bulk carrier density. The difference between n_0 and N_+ arises from the deep bulk tarp.

Let

$$ \frac{N_{\rm d}A}{n_0}\left(\frac{\varepsilon\varepsilon_0 eN_+}{2\Phi_{\rm B}}\right)^{1/2} = \lambda,$$

we can obtain ${\rm d}Q = \lambda {\rm d}V$. Under AC signal, ${\rm d}V(t) = {\rm d}V{\rm e}^{{\rm i}\,\omega t}$, the current is given by

$$ j_{\rm d}(t) = -\frac{{\rm d}Q(t)}{{\rm d}t} = e_{\rm n}Q(t), \tag{14}$$

where $e_{\rm n}$ is the emission rate of the trap.

As $Q(t) = {\rm d}Q(t) - \int_0^t j_{\rm d}(t){\rm d}t$, we get $j_{\rm d}(t) = e_{\rm n}[{\rm d}Q(t) - \int_0^t j_{\rm d}(t){\rm d}t]$, so

$$ j_{\rm d}(t) = e_{\rm n}\left[\lambda {\rm d}V(t) - \int_0^t j_{\rm d}(t){\rm d}t\right]. \tag{15}$$

Let $\tan\theta = e_{\rm n}/\omega$, we can obtain the solution as

$$ j_{\rm d}(t) = \lambda e_{\rm n}\cos\theta {\rm d}V\exp[{\rm i}(\omega t + \theta)]. \tag{16}$$

So $j_{\rm d}$ is out of phase with the signal, and can be written as two components: one in phase $j_{\rm phase}$ and the other in quadrature $j_{\rm quad}$,

$$ j_{\rm phase} = \frac{\lambda e_{\rm n}\omega^2}{e_{\rm n}^2 + \omega^2}{\rm d}V\exp({\rm i}\,\omega t), \tag{17}$$

$$ j_{\rm quad} = \frac{\lambda e_{\rm n}^2\omega}{e_{\rm n}^2 + \omega^2}{\rm d}V\exp\left[{\rm i}\left(\omega t + \frac{\pi}{2}\right)\right]. \tag{18}$$

The admittance $Y = j/{\rm d}V = G + {\rm i}\,\omega C$, can be presented by G and C

$$ G = \frac{|j_{\rm phase}|}{{\rm d}V} = \frac{\lambda e_{\rm n}\omega^2}{e_{\rm n}^2 + \omega^2}, \tag{19}$$

$$ C = \frac{|j_{\rm quad}|}{\omega {\rm d}V} = \frac{\lambda e_{\rm n}^2}{e_{\rm n}^2 + \omega^2}. \tag{20}$$

At high frequency, the barrier is analogous to parallel plate capacitor with a plate separation corresponding to the total depletion width sandwiched between the well conducting grains[12]

$$ C_{\rm HF} = \frac{\varepsilon\varepsilon_0 A}{x_0} = A\left(\frac{\varepsilon\varepsilon_0 eN_+}{2\Phi_{\rm B}}\right)^{1/2}. \tag{21}$$

Thus $\lambda = C_{\rm HF}N_{\rm d}/n_0$, and

$$ G = C_{\rm HF}\frac{N_{\rm d}}{n_0}\frac{e_{\rm n}\omega^2}{e_{\rm n}^2 + \omega^2}, \tag{22}$$

$$ C = C_{\rm HF}\frac{N_{\rm d}}{n_0}\frac{e_{\rm n}^2}{e_{\rm n}^2 + \omega^2}. \tag{23}$$

It can be seen from Eqs. (22) and (23) that the relationship between G, C and ω is of Debye type. So the electron trapping and emitting by deep bulk trap is a Debye-type relaxation, with a relaxation time $\tau = 1/e_{\rm n}$.[12,15]

The relationship between emission rate and temperature is

$$ e_{\rm n} = e_{\rm n0}\exp[(E_{\rm d} - E_{\rm c})/kT]. \tag{24}$$

The G has a maximum when $e_{\rm n} = \omega$, at a temperature

$$ T_{\rm m} = [(E_{\rm d} - E_{\rm c})/kT][\ln(\omega/e_{\rm n0})]^{-1}. \tag{25}$$

Namely

$$ \ln\omega = [(E_{\rm d} - E_{\rm c})/kT]\frac{1}{T_{\rm m}} + \ln e_{\rm n0}. \tag{26}$$

Thus the energy level of deep bulk trap $E_{\rm d}$ can be obtained from the $\ln(\omega) \sim 1/T_{\rm m}$ curve.

Considering the DC conductance and k kind of deep bulk trap, we can write the conductance as

$$G = G_0 + C_{\rm HF} \sum_{i=1}^{k} \frac{N_{\rm di}}{n_0} \frac{e_{\rm ni}\omega^2}{e_{\rm ni}^2 + \omega^2}. \tag{27}$$

From the experimental result shown in Fig. 5, two resonances can be seen obviously on the curves of conductivity versus temperature even when the bias is zero, and they nearly change with bias, as shown in Fig. 7 when the frequency is 10^5 Hz.

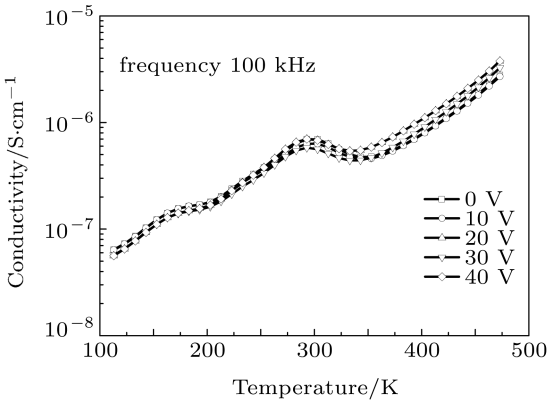


Fig. 7. Deep bulk trap relaxation on conductance versus temperature curve at 10^5 Hz and various values of bias.

According to Eq. (26), the activation energy can be obtained from the slope of $\ln f \sim 1000/T_{\rm m}$ curve, as shown in Fig. 8 when the bias is zero.

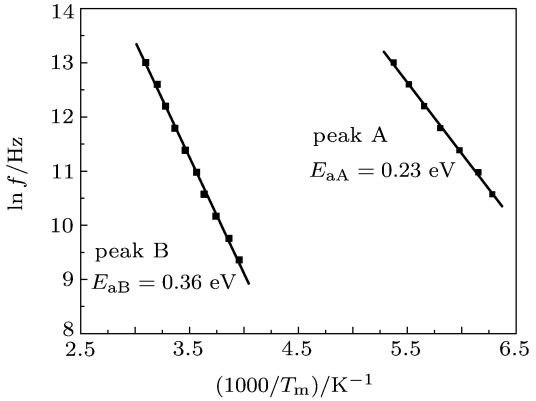


Fig. 8. The $\ln f \sim 1000/T_{\rm m}$ curve obtained from deep bulk trap relaxation resonances on dielectric spectra shown in Fig. 5(a).

The activation energy also hardly changes with the bias, as listed in Table 1, so the deep bulk trap relaxation at the edge of depletion layers is independent of the bias, only depends on the nature of the trap itself. Generally, in the depletion layer, main defects are positively charged ions, including the stable trivalent substitutional ions, oxygen vacancies and sub-stable interstitial Zn ions. As the value of the activation energy is about 0.22 eV and 0.35 eV, which is close to the electronic energy level of native defect interstitial zinc and oxygen vacancy,[2,15] it can be concluded that the relaxation at zero bias comes from the relaxation of deep bulk trap, interstitial zinc and oxygen vacancy at the edge of depletion layers.

Table 1. Activation energy of deep bulk trap relaxation at different bias calculated from resonances on dielectric spectra.

bias/V	0	10	20	30	40
peak A $E_{\rm a}$/eV	0.23	0.24	0.20	0.22	0.23
peak B $E_{\rm a}$/eV	0.36	0.35	0.31	0.34	0.34

Besides the activation energy of deep bulk trap relaxation in depletion layers, the emission rate can also be obtained from the intercept of $\ln f \sim 1000/T_{\rm m}$ curve based on Eq. (26), and the trap density can be obtained from the peak value of G.

3.5. Interface relaxation

As the bias is not zero, the barrier is no longer symmetric, so electron trapping and emitting by interface states are not instantaneous, leading to the change of interface charge. When the interface charge changes, the barrier height will change, thus additional current will flow over the barrier, exhibiting as a resonance on the dielectric spectra.

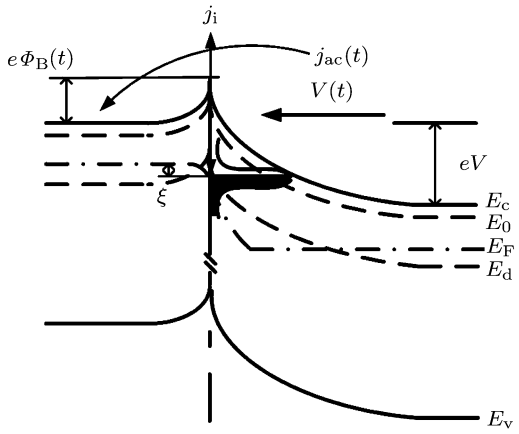


Fig. 9. Schematic diagram of interface relaxation under non-zero bias small AC signal. Additional current rising from interface state relaxation $j_{\rm i}$ is shown. The barrier height $\Phi_{\rm B}(t)$ and net current flowing through the barrier $j_{\rm ac}(t)$ become time-dependent.

As the grain boundary is under a small AC signal $V(t) = V_0 + V{\rm e}^{{\rm i}\omega t}$, $eV \ll kT$, the time dependence barrier height can be written as $\Phi_{\rm B}(t) = \Phi_{\rm B} - {\rm d}\Phi_{\rm B}(t)$. As discussed in Section 2, in the steady state condition, the net current through the barrier can be approximated as thermionic emission current j written

as Eq. (8). While under the small AC signal, due to the change of barrier height, an additional current should be involved in the net current through the barrier, namely

$$\begin{aligned} \mathrm{d}j_{\mathrm{ac}}(t) &= AT^2 \exp\{-e[\Phi_{\mathrm{B}}(V) - \mathrm{d}\Phi_{\mathrm{B}}(t)]/kT\} \\ &= j_{\mathrm{dc}} \exp[e\mathrm{d}\Phi_{\mathrm{B}}(t)/kT]. \end{aligned} \tag{28}$$

It can be seen that the additional current $\mathrm{d}j_{\mathrm{ac}}(t)$ is not in phase with $\mathrm{d}V(t)$, but depends exponentially on $\mathrm{d}\Phi_{\mathrm{B}}(t)$, this out-of-phase modulation of the barrier height can give rise to a large capacitive current proportional to j_{dc}.

As $\mathrm{d}\Phi_{\mathrm{B}}(t)$ is determined by charge neutrality condition, the relationship between $\mathrm{d}\Phi_{\mathrm{B}}(t)$ and $\mathrm{d}V(t)$ can be obtained by interface charge equilibrium. As $Y_{\mathrm{i}} = \mathrm{d}j_{\mathrm{ac}}/\mathrm{d}V(t) = G_{\mathrm{i}} + \mathrm{i}\,\omega C_{\mathrm{i}}$, the equivalent conductance and capacitance rising from the interface relaxation can be obtained and verified to be of Debye type, with the relaxation time τ_{i} given as[12,16,24]

$$\tau_{\mathrm{i}} = \frac{e}{2AT^2c} \frac{\exp[(e\Phi_{\mathrm{B0}} + \varepsilon_\xi)/kT]}{1 + \exp(-eV_0/kT)}. \tag{29}$$

As the relaxation time τ_{i} decreases with increasing bias, when the bias is zero or not high enough, the relaxation time is too long to be detected in measuring frequency range. In addition, from the resonance on the dielectric spectra, we cannot obtain the energy level of interface states, which is independent of the relaxation time τ_{i}. Temperature is involved both in numerator and denominator, so the variation of relaxation time τ_{i} with temperature is not so obvious.

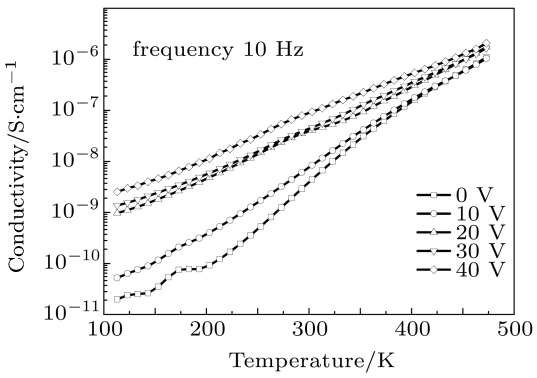


Fig. 10. Interface relaxation on conductance versus temperature curve at 10 Hz and various values of bias.

From the dielectric spectra shown in Fig. 5, we can see that the resonance appears on the conductance–temperature curve near 300 K, under non-zero bias. This resonance can only be observed in low frequency region, and is most obvious when the bias is 20 V as shown in Fig. 10 when the frequency is 10 Hz. As we discussed above, when the bias is less than 20 V, relaxation time is too long due to the high barrier height; while the bias is higher than 20 V, the resonance is superposed with DC conductance, which increases with increasing bias, so the resonance is concealed at high bias.

3.6. The DC-like conductance

In the high temperature region, the $\ln G \sim 1000/T$ curve is almost a straight line, which is the same as DC conductance. But in the temperature range of 160 °C∼200 °C at the frequency of 10 Hz, the activation energy is 0.48 eV, which is much less than the barrier height 0.69 eV obtained in steady state. This may be attributed to the effect of relaxation conductance, which presents like a peak and declines at high temperature, leading to lower activation energy. But this effect is not so significant, a more advisable reason is that the high temperature region conductance is different from DC conductance in nature. Under AC signal, conductance comes not only from charge transportation between electrodes, as the steady state; on the other hand, displacement of charge can also give rise to dielectric loss, which presents as conductance in dielectric spectra, although there is no other resonance in our measurement region, we cannot represent the nature of this relaxation, which may come from the shallow bulk trap or other factors

4. Conclusions

In this paper, the steady state and dynamic response of ZnO ceramics are investigated theoretically and experimentally, especially by dielectric spectroscopy.

In a steady state condition, the nature of net current flow over the barrier was discussed by considering the interface trapping and emitting, quasi-Fermi level difference between the interface and bulk Fermi level and the reverse current. Approximate calculation was carried on, and temperature-dependent barrier height was obtained from the steady I–V characteristics.

As for the dynamic response, the additional conductance and capacitance coming from deep bulk trap relaxation were calculated based on the displacement of the cross point between deep bulk trap and Fermi level under small AC signal. Resonances due to deep bulk trap relaxation are shown on dielectric spectra, even when the bias is zero. From the slope of $\ln f \sim 1000/T_{\mathrm{m}}$ curve, the activation energies are obtained as 0.22 eV and 0.35 eV, which are consistent with the electronic level of the main defect interstitial Zn and vacancy oxygen in the depletion layer. Under moderate bias, another resonance due to interface relaxation is shown on the dielectric spectra. Because of

the barrier height dependence of long relaxation time $\tau_{\rm i}$, and the superposition with DC conductance in high temperature region, interface relaxation can only be observed in special frequency and temperature region under moderate bias.

In addition, the DC-like conductance is obtained from the dielectric spectra in high temperature region, and the activation energy is much smaller than the barrier height in steady state condition. So we can say that displacement current coming from the shallow bulk trap relaxation or other factors contributes a lot to the total conductance under small AC signal. In conclusion, we can obtain temperature-dependent barrier height from the steady I–V characteristics; whereas the electronic level of the main defect interstitial Zn and vacancy oxygen in the depletion layer can be obtained from dielectric spectra of ZnO ceramics. All these can give lots of guidance to engineering application. As interstitial Zn has a great effect on the degradation of ZnO varistor,[3] from the dielectric spectra, we can easily obtain information about interstitial Zn, and then judge the degradation characteristics. In high-current region ($j > 10^2$ A/cm^2),[1] the grain boundaries are broken down by tunneling effect, the residual voltage is attributed to the resistance of grains and the voltage drop of the grain boundary, and the latter is quite dependent on interface state. As we can obtain the information about interface state from the interface relaxation showing up on dielectric spectra, interface state can be easily detected. After it is properly controlled, the residual voltage of ZnO varistor can be declined, although further study is needed.

References

[1] Clarke D R 1999 *J. Am. Ceram. Soc.* **82** 485

[2] Gupta T K 1990 *J. Am. Ceram. Soc.* **73** 1817

[3] Eda K 1989 *Electrical Insulation Magazine IEEE* **5** 28

[4] Peng C X, Wang K F and Zhang Y 2009 *Chin. Phys.* B **18** 2072

[5] Wen X M, Ohno N and Zhang Z M 2001 *Chin. Phys.* **10** 874

[6] Pike G E and Seager C H 1979 *J. Appl. Phys.* **50** 3414

[7] Morris W G 1976 *J. Vac. Sci. Technol.* **13** 926

[8] Emtage P R 1977 *J. Appl. Phys.* **48** 4372

[9] Eda K 1978 *J. Appl. Phys.* **49** 2964

[10] Mahan G D, Lionel M L and Philipp H R 1979 *J. Appl. Phys.* **50** 2799

[11] Pike G E 1982 *Mater. Res. Soc. Proc.* **5** 369

[12] Greuter F and Blatter G 1990 *Semicond. Sci. Technol.* **5** 111

[13] Werner J, Ploog K and Queisser H J 1986 *Phys. Rev. Lett.* **57** 1080

[14] Han J, Senos A M R and Mantas P Q 2003 *J. Appl. Phys.* **93** 4097

[15] Cheng P F, Li S T and Zhang L 2008 *Appl. Phys. Lett.* **93** 012902

[16] Blatter G and Greuter F 1986 *Phys. Rev.* B **33** 3952

[17] Levinson L M and Philipp H R 1977 *IEEE Transactions on Parts, Hybrids and Packaging* **PHP-13** 338

[18] Levinson L M and Philipp H R 1976 *J. Appl. Phys.* **47** 1117

[19] Levinson L M and Philipp H R 1978 *J. Appl. Phys.* **49** 6142

[20] Alim M, Li S T and Liu F Y 2006 *Phys. Stat. Sol.* (a) **203** 410

[21] Li S T, Yang Y and Zhang L 2009 *Chin. Phys. Lett.* **26** 077201

[22] Li S T, Yang Y and Zhang L 2009 *Acta Phys. Sin.* **58** 264 (in Chinese)

[23] Vincent G, Bois D and Pinard P 1975 *J. Appl. Phys.* **46** 5173

[24] Seager C H and Pike G E 1980 *Appl. Phys. Lett.* **37** 747